



MAŁGORZATA LALAK-DYBAŁA

WSEI University in Lublin, Poland

ORCID iD: orcid.org/0000-0001-5694-3460

BARBARA STEFANIAK

Netrix S.A., Poland

ORCID iD: orcid.org/0000-0001-6555-8230

PAWEŁ OLSZEWSKI

WSEI University in Lublin, Poland

ORCID iD: orcid.org/0000-0002-1015-1190

ANALYSIS OF THE EFFECTIVENESS OF TWO DIFFERENT LOSS FUNCTIONS IN TRAINING A NEURAL NETWORK IN LUNG IMAGE RECONSTRUCTION USING IMPEDANCE TOMOGRAPHY

ANALIZA SKUTECZNOŚCI DWÓCH RÓŻNYCH FUNKCJI STRAT W PROCESIE TRENOWANIA SIECI NEURONOWEJ W REKONSTRUKCJA OBRAZÓW PŁUC Z WYKORZYSTANIEM TOMOGRAFII IMPEDANCYJNEJ

ABSTRACT

The article presents research findings on developing a medical diagnostic system based on electrical impedance tomography technology. One of the key components of this project is developing a method for reconstructing the structure of human lungs using this technology. The authors of the article compared the effectiveness of two different loss functions in training a neural network, which is tasked with accurately replicating the lung structure based on electrical impedance tomography data.

The researchers analyzed various approaches to calculating loss functions, including cosine embedding loss and InfoNCE loss. They compared the results obtained using these two functions to identify which one performs better in lung structure reconstruction. The findings of these studies may have significant implications for the development of diagnostic systems based on electrical impedance tomography and for improving the effectiveness of lung disease diagnosis.

Additionally, the authors discuss potential future directions for the project, including possible applications of the research findings in clinical practice. Future research efforts may focus on optimizing neural network parameters, exploring alternative loss functions, or utilizing advanced machine learning techniques for even more precise lung structure reconstruction. The pursuit of improving such diagnostic systems could lead to significant advancements in the field of medicine, particularly in diagnosing and treating respiratory diseases.

STRESZCZENIE

Artykuł przedstawia wyniki badań związanych z projektowaniem systemu diagnostycznego opartego na technologii elektrycznej tomografii impedancyjnej. Jednym z głównych elementów tego projektu jest opracowanie metody rekonstrukcji struktury ludzkich płuc przy użyciu tej technologii. Autorzy artykułu przeprowadzili porównanie skuteczności dwóch różnych funkcji strat w procesie trenowania sieci neuronowej, która ma za zadanie dokładnie odwzorować strukturę płuc na podstawie danych z tomografii impedancyjnej elektrycznej.

Badacze analizowali różne podejścia do obliczania funkcji strat, w tym stratę kosinusowego wbudowania oraz stratę informacyjną InfoNCE. Porównanie wyników uzyskanych przy użyciu tych dwóch funkcji miało na celu zidentyfikowanie, która z nich lepiej sprawdza się w procesie rekonstrukcji struktury płuc. Wyniki tych badań mogą mieć istotne znaczenie dla rozwoju systemów diagnostycznych opartych na tomografii impedancyjnej elektrycznej oraz dla poprawy skuteczności diagnozowania chorób płuc.

Dodatkowo, autorzy omawiają możliwe dalsze kierunki rozwoju projektu, w tym potencjalne zastosowania wyników badań w praktyce klinicznej. Przyszłe prace badawcze mogą skupić się na optymalizacji parametrów sieci neuronowej, eksploracji innych funkcji strat lub wykorzystaniu zaawansowanych technik uczenia maszynowego w celu jeszcze dokładniejszej rekonstrukcji struktury płuc. Dążenie do doskonalenia tego typu systemów diagnostycznych może prowadzić do znacznego postępu w dziedzinie medycyny, szczególnie w diagnostyce i leczeniu chorób układu oddechowego.

KEYWORDS: Electrical impedance tomography, Lung reconstruction, convolutional neural network, neural network with encoder-decoder architecture, ResNet

SŁOWA KLUCZOWE: *Elektryczna impedancyjna tomografia, rekonstrukcja płuc, sieci konwolucyjne, sieci neuronowe z architekturą endocer-decoder, ResNet*

INTRODUCTION

In the era of technological and medical advancement, lung image reconstruction has become a crucial medical diagnostic, therapeutic, and research tool. The multifaceted application of this advanced imaging process plays a fundamental role in identifying, treating, and monitoring lung diseases, especially in the context of evolving global health challenges (Li, 2023).

Various medical tests are employed to diagnose diseases such as chest computer tomography, spirometry, arterial blood gas analysis, pulmonary imaging, biomarkers in alveolar fluid, lung ultrasonography, chest X-ray, and bronchial provocation tests such as those involving methacholine or histamine. To undergo the mentioned examinations, patients must follow specific instructions and be guided on proper behavior during the procedure. Occasionally, test results may not be immediately available, as they might require analysis and description by the relevant medical professional, which can take some time. However, a solution that enables an approximate diagnosis within just a few minutes will be presented. We will present electric impedance tomography as an alternative to these examinations (Gray, 2021).

Electrical Impedance Tomography (EIT) represents cutting-edge technology in lung imaging. This method relies on measuring electrical voltages across points and surface electrodes, offering remarkable time resolution for real-time tracking of changes. EIT is notably non-invasive, with minimal side effects such as no radiation exposure or patient transport requirements (Filipowicz, 2023).

The article presents a detailed 2D model of a male torso, with a specific focus on depicting the lungs. The lungs are segmented into three distinct sub-areas: bronchi/bronchioles, blood vessels/capillaries surrounding the bronchi, and

lung tissue. The paper showcases 2D reconstructions generated by specialized neural networks using impedance tomography measurements. The training dataset includes lung images captured across various breathing phases and comprises ninety shapes. To simulate noise from the measurement device, proportional Gaussian noise at a level of 5% was added to the simulated voltages.

RESEARCH METHODOLOGY

EIT is an imaging method that employs electrical impedance measurement inside the patient's body to visualize the lung structure. Constructing a male torso model is based on the analysis of computed tomography (CT) images, which allow for precise visualization of anatomical details (Meerburg, 2020).

The first step involves segmentation, which extracts the torso and lungs from the image background using a two-level thresholding process. Subsequently, a more detailed segmentation is performed to extract the bronchi/bronchioles. For this purpose, the Otsu method (Goh, 2018) is applied to the area with the extracted lungs. Additionally, the structure of blood vessels/capillaries surrounding the bronchi in the lungs is simulated using a morphological operation called dilation with a structural element in the shape of a unit circle.

In the first stage, an EIT model is defined. The mesh configuration comprises 16-point electrodes positioned along the torso's boundary, comprising 6062 elements and 3160 nodes. A triangular mesh is determined based on the labelled image (labels from 1 to 6 in Table 1), where pixels are divided into two triangles (Figure 1 presents the labelled mesh). Subsequently, the distribution on a slice of the human torso is simulated (Filipowicz, 2003).

The second stage involves simulating the permeability distribution on a slice of the human torso. Table 1 presents tissue values for the human lung model. Then, a dataset is calculated for the neural network. The dataset is derived from EIT measurements employing a bipolar stimulation pattern. Simulated measurements are obtained using the finite element method (FEM).

Table 1. *Material parameter for distracted fields on mesh*

Area name	Area index	Material parameter	Normalized material parameter
Torso	1	0.4610	1
Left lung	2	0.1111	0.2410
Right lung	3	0.1111	0.2410
Lungs Bronchi	4	10^{-10}	$2.2 \cdot 10^{-10}$
Blood vessels along the bronchi	5	0.6625	1.4370

Source: (Hasgall, 2022)

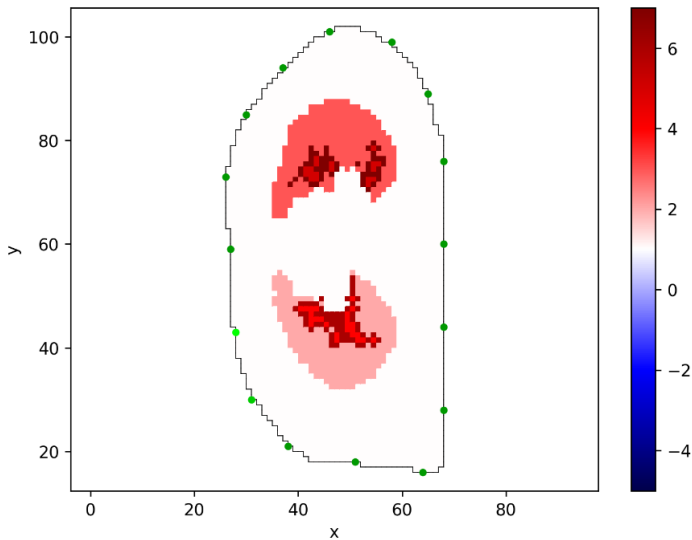
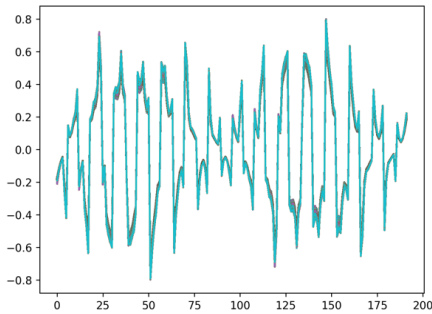
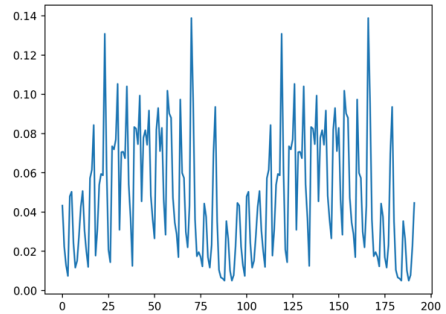
Figure 1. *Distribution tissues of torse model on a triangle mesh*

Figure 2 depicts 50,000 measurement cases, while Figure 3 presents the variability of values for each measurement index. It's worth noting that there is little variability for each measurement. The highest variability is around 0.14, and the lowest is around 0.01, with values in the range of 0.8. The neural network's task will be to distinguish between individual measurements and transform them into a vector of length 6062, illustrating the reconstruction on the grid depicted in Figure 1.

Figure 2. Calculate measurement**Figure 3.** Range of each index of measurement

NEURAL NETWORK WITH ARCHITECTURE ENCODER-DECODER (HE, 2016)

ResNet, or Residual Neural Network, is a groundbreaking architecture in deep learning, particularly in image recognition and classification. Introduced by Kaiming He et al. in their paper *Deep Residual Learning for Image Recognition* in 2015, ResNet addressed the problem of vanishing gradients in deep neural networks, allowing for the training of significantly deeper models (Wójcik, 2024).

The core innovation of ResNet lies in introducing skip connections, also known as residual connections, which enable the network to bypass specific layers during training. These connections allow the model to learn residual mappings rather than directly attempting to understand the desired underlying mapping. As a result, ResNet can effectively train extremely deep networks (e.g., hundreds of layers) without encountering issues such as performance degradation caused by the vanishing gradient problem.

The architecture of ResNet typically consists of a series of convolutional layers followed by batch normalization and rectified linear unit (ReLU) activations, along with residual blocks containing skip connections. These residual blocks are the building blocks of the network and can be stacked to create deeper architectures. ResNet has achieved state-of-the-art performance on various image classification tasks, winning the ImageNet Large Scale Visual Recognition

Challenge (ILSVRC) in 2015. Its success has led to widespread adoption and is the basis for many subsequent advancements in deep learning architectures (Kłosowski, 2023; Miciura, 2024). Lungs were represented by two networks with architecture like ResNet and different loss functions for reconstruction.

LOSS FUNCTIONS

The Cosine Embedding Loss is a widespread loss function used in deep learning, particularly in metric and similarity learning tasks. It is designed to optimize the embedding space such that similar samples are pulled closer together while dissimilar samples are pushed apart. This loss function is particularly effective in scenarios where the similarity between samples is essential, such as face recognition or information retrieval tasks.

At its core, the Cosine Embedding Loss measures the cosine similarity between pairs of embeddings in the feature space. It encourages embeddings of similar samples to have a cosine similarity close to 1, indicating high similarity. In contrast, embeddings of dissimilar samples should have a cosine similarity close to -1 , indicating dissimilarity. This approach allows for the training of deep neural networks to learn discriminative representations that capture the underlying similarity structure of the data (Hsu, 2022).

One of the key advantages of the Cosine Embedding Loss is its robustness to changes in the scale and magnitude of the embeddings. Unlike Euclidean distance-based losses, such as contrastive loss or triplet loss, the cosine similarity is invariant to the magnitude of the embeddings, focusing solely on the direction of the vectors. This property makes the Cosine Embedding Loss particularly well-suited for tasks where the absolute magnitude of the embeddings is not meaningful, such as in image classification or semantic similarity tasks (Kovacs, 2015).

InfoNCE Loss, or Info Normalized Cross Entropy Loss, is an innovative loss function used in representation and self-supervised learning approaches in deep neural networks. It is an alternative to traditional loss functions that rely on class labels or distances between examples.

InfoNCE Loss is based on the concept of information encoding channels derived from information theory. It involves maximizing the mutual information

between positive and negative examples in the embedding space. In other words, the loss function aims to maximize the differences in probability distributions between correct and false pairs of examples (Pielawski, 2020).

The InfoNCE loss function is used with contrastive neural network architectures such as Contrastive Predictive Coding (CPC) or Contrastive Autoencoder Network (CAN). It is employed to learn features in custom unsupervised learning tasks, such as generating representations with annotated and artificially generated negative examples. This approach is beneficial in domains where traditional labels are missing or insufficient, and networks must learn meaningful features autonomously (Van den Oord, 2019).

The choice of these two loss functions reflects the desire to leverage their respective strengths in encouraging the neural network to learn representations that accurately capture the complex structure of the lungs based on electrical impedance tomography (EIT) data. Comparing the performance of these two loss functions provides insights into which approach is more effective for the specific task and can potentially improve the accuracy of lung structure reconstruction in diagnostic applications.

RESULTS

Figures 4, 5, and 6 showcase a sample output of the network's operation with the cosine embedding loss function. In Figure 4, a visualization of the simulated permeability distribution is presented, with Gaussian noise added proportionally to the data at a level of 5%. Figure 5 illustrates the reconstruction, while Figure 6 displays the absolute difference between the simulation and the reconstruction. The reconstruction portrays a denoised image, with the most significant errors observed at the boundaries of value changes.

In image reconstruction, the network aims to accurately recreate the underlying structure while minimizing the impact of noise introduced during simulation. Adding Gaussian noise simulates real-world conditions and challenges faced in practical applications. By visualizing the difference between the simulated distribution and the reconstructed image, analysts can assess the effectiveness of the network in capturing and representing the essential

features of the original data. Furthermore, identifying areas of high error can guide improvements in the network architecture or training process to enhance the accuracy of future reconstructions.

Figure 4. *Simulation*

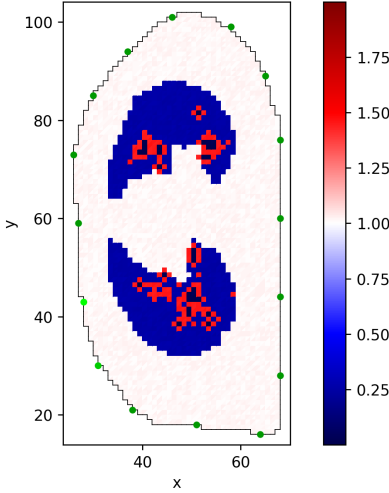


Figure 5. *Reconstruction*

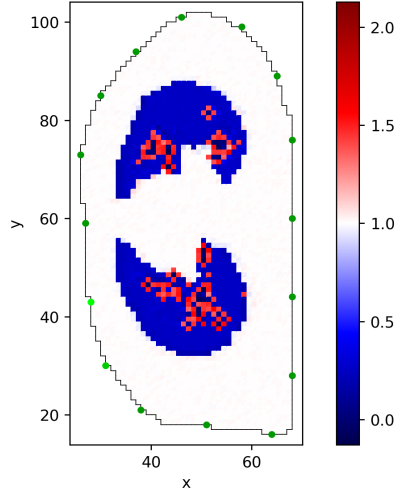
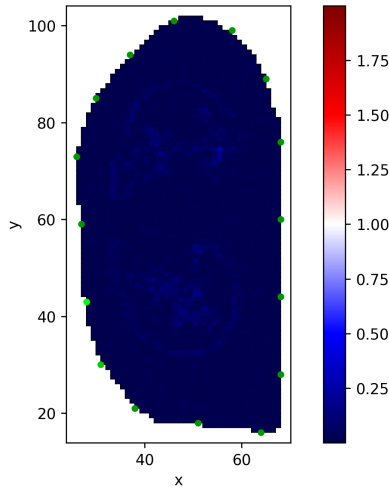


Figure 6. *The absolute difference between reconstruction and simulation*



Figures 7, 8, 9, and 10 provide an in-depth illustration of the network's performance when utilizing the InfoNCE loss function. Figure 7 showcases the simulated permeability distribution, mirroring the visualization depicted in Figure 4. Figure 8 displays the reconstruction process employing the neural network with the InfoNCE loss function. Meanwhile, Figure 9, akin to Figure 6, presents the absolute disparity between the simulated distribution and the reconstructed image. Figure 10 exhibits the absolute difference between the reconstruction and simulation in a 1D space for a more precise depiction of errors.

Through this analysis, we aim to evaluate the efficacy of the network in capturing the underlying structure while mitigating the impact of noise. Applying the InfoNCE loss function facilitates learning meaningful representations, enhancing the network's ability to produce accurate reconstructions. By visualising the absolute differences, analysts can pinpoint areas of discrepancy and assess the network's performance in detail. Notably, the maximum absolute error observed in Figure 10 is approximately 0.0375, indicative of the network's capability to achieve precise reconstructions with minimal error.

Figure 7. *Example simulation*

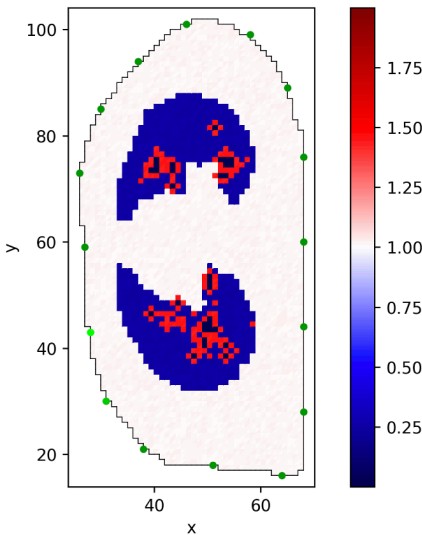


Figure 8. *Example reconstruction with the neural network with InfoNCE loss*

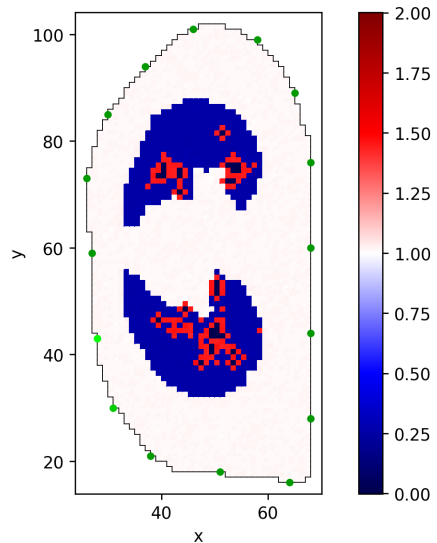


Figure 9. *Absolute difference reconstruction and simulation*

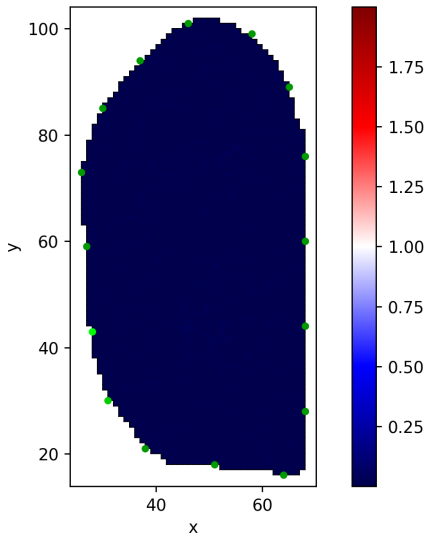


Figure 10. *The absolute difference between reconstruction and simulation in 1D space*

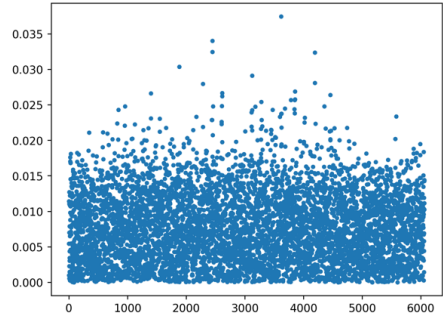


Table 2 compares coefficients for two different loss functions utilized in the neural network model. The table includes the Pearson coefficient, the linear correlation between two variables, and the mean-squared error (MSE) for the reconstruction process.

For the Cosine Embedding loss function, the Pearson coefficient is calculated to be 0.99716, indicating a robust positive linear correlation between the predicted and actual values. Additionally, the MSE for the reconstruction is 0.045653697, representing the average squared difference between the expected and actual values.

On the other hand, for the InfoNCE loss function, the Pearson coefficient is 0.75998, indicating a positive correlation between the predicted and actual values, albeit not as strong as with the Cosine Embedding loss function. The MSE for the reconstruction is 0.03208109, suggesting a lower average squared difference between the predicted and actual values compared to the Cosine Embedding loss function.

Overall, the table provides a quantitative comparison of the performance of the two loss functions in terms of their ability to generate accurate reconstructions and their correlation with the actual values.

Table 2. Compare coefficients for two loss functions

Loss function	Pearson coefficient	MSE reconstruction
Cosine embedding	0.99716	0.045653697
InfoNCE	0.75998	0.03208109

CONCLUSIONS

In the presented analysis, the effectiveness of two different loss functions was compared in terms of their impact on the operation of the neural network model. The first of the examined functions was the cosine embedding loss, demonstrating a strong positive linear correlation (Pearson coefficient = 0.99716) between predicted and actual values. The MSE for the reconstruction process was 0.045653697, suggesting that the model achieved high accuracy in generating reconstructions.

On the other hand, the InfoNCE loss function showed a slightly weaker but still positive linear correlation (Pearson coefficient = 0.75998) between predicted and actual values. The MSE for this loss function was 0.03208109, indicating lower average squared differences between expected and actual values compared to the cosine embedding loss function.

The results suggest that the cosine embedding loss function achieved better outcomes in generating more accurate reconstructions due to its higher linear correlation and slightly higher MSE. However, the InfoNCE loss function also demonstrated good effectiveness, suggesting that it may be helpful in other contexts or for different purposes. Ultimately, the choice of loss function should be carefully considered, considering the specifics of the problem and expectations regarding the quality of generated reconstructions.

This methodology enables precise delineation of pulmonary structure and its constituent elements, offering significant potential for enhancing diagnostic, therapeutic, and monitoring capabilities in lung diseases. Future advancements

in this field could leverage artificial intelligence and machine learning techniques to refine and automate image reconstruction, potentially leading to even more accurate and efficient diagnoses (Rymarczyk, 2019). Additionally, integrating real-time data analytics and telemedicine technologies could facilitate remote monitoring and consultation, extending access to specialized care for patients in remote or underserved areas. Moreover, continued research into novel imaging modalities and biomarkers may unlock new insights into lung pathophysiology, enabling earlier detection and personalized treatment strategies. Overall, the ongoing evolution of lung imaging techniques holds promise for improving patient outcomes and advancing the understanding and management of respiratory conditions.

REFERENCES

- Filipowicz, S.F., Rymarczyk, T., (2003). Tomografia impedancyjna, pomiary, konstrukcje i metody tworzenia obrazu: 95-101
- Goh, T. Y., Basah, S. N., Yazid, H., Safar, M. J. A., Saad F. S. A., (2018). 'Performance Analysis of Image Thresholding: Otsu Technique'. *Measurement* 114 (1 January 2018): 298–307. <https://doi.org/10.1016/j.measurement.2017.09.052>.
- Gray, D. M., Owusu, S.K., Van der Zalm M. M., (2021). 'Chronic Lung Disease in Children: Disease Focused Use of Lung Function'. *Current Opinion in Physiology* 22 (1 August 2021): 100438. <https://doi.org/10.1016/j.cophys.2021.05.001>.
- Hasgall, P.A., Gennaro, Di. F., C. Baumgartner, Neufeld, E., Lloyd, B., Gosselin, M. C., Payne, D., Klingenböck, A., Kuster, N., (2022). *IT'IS Database for thermal and electromagnetic parameters of biological tissues*, Version 4.1.
- He, K., Zhang, X., Ren, S., Sun, J., (2016). *Deep Residual Learning for Image Recognition*, IEEE Conference on Computer Vision and Pattern Recognition (CVPR).
- Hsu, Gee-Sern J., Wu, H. Y., Tsai, C. H., Yanushkevich, S., Gavrilova. M. L., (2022). 'Masked Face Recognition From Synthesis to Reality'. *IEEE Access* 10 (2022): 37938–52. <https://doi.org/10.1109/ACCESS.2022.3160828>
- Kłowski, G., Rymarczyk, T., Wójcik, D., (2023). 'The Use of an LSTM-Based Autoencoder for Measurement Denoising in Process Tomography'. *International Journal of Applied Electromagnetics and Mechanics* 73, no. 4 (1 January 2023): 339–52. <https://doi.org/10.3233/JAE-230013>
- Kovács, B., Reiner, P., (2019). Akihiro Sugimoto, *Deep Metric Learning using Triplet Network*, 42nd International Conference on Telecommunications and Signal Processing.
- Li, X., Zhang, R., Wang, O., Duan, X., Sun, Y., Wang, J., (2023). 'SAR-CGAN: Improved Generative Adversarial Network for EIT Reconstruction of Lung Diseases'. *Biomedical Signal Processing and Control* 81 (1 March 2023): 104421. <https://doi.org/10.1016/j.bspc.2022.104421>
- Maciura, Ł., Rymarczyk, T., Wójcik, D., Gauda, K., Kowalski, M., (2024). 'Deep Learning Correction for Image Reconstruction in Electrical Impedance Tomography Using UNet Model. | Przegląd Elektrotechniczny | EBSCOhost'. Accessed 28 April 2024. <https://openurl.ebsco.com/EPDB%3Agcd%3A1%3A28642033/detailv2?sid=ebsco%3Aplink%3A scholar&tid=ebsco%3Agcd%3A164567736&crl=c>
- Meerburg, J. J., Veerman, G. D. M., Aliberti, Tiddens. S., H. A. W. M., (2020). 'Diagnosis and Quantification of Bronchiectasis Using Computed Tomography or Magnetic Resonance Imaging: A Systematic Review'. *Respiratory Medicine* 170 (1 August 2020): 105954. <https://doi.org/10.1016/j.rmed.2020.105954>
- Pielawski, N., Wetzer, E., Öfverstedt, J., Lu, J., Wählby, C., Lindblad, J., Sladoje, N., (2020). 'CoMIR: Contrastive Multimodal Image Representation for Registration'. *Advances in Neural Information Processing Systems 2020-December* (2020): undefined-undefined. <https://www.mendeley.com/catalogue/29145d83-6a07-323f-8bfc-fc875dda66cf/>

- Rymarczyk, T., (2019). ‘Wearable Mobile Measuring Device Based on Electrical Tomography’. PRZEGLĄD ELEKTROTECHNICZNY 1, no. 4 (5 April 2019): 213–16. <https://doi.org/10.15199/48.2019.04.39>
- Wójcik, D., Rymarczyk, T., Maciura, Ł., Oleszek, M., Adamkiewicz, P., (2024). ‘Time Series Recognition with Convolutional and Recursive Neural Networks in BSPM | IEEE Conference Publication | IEEE Xplore’. Accessed 28 April 2024. <https://ieeexplore.ieee.org/abstract/document/10124427>
- Van den Oord, A., Li, Y., Vinyals, O.,(2019). *Representation Learning with Contrastive Predictive Coding* arXiv.